PhotoScience Advances
https://www.sciltp.com/journals/psa

Article

Initiation of Radical Photopolymerization with Perylenebisimide Derivatives Having Twisted Molecular Structures as Heavy-Atom-Free Visible Light-Harvesting Efficient Photoinitiators

Wenhui Li [1], Yuqi Hou [2] and Jianzhang Zhao [1,*]

[1] State Key Laboratory of Fine Chemicals, Frontiers Science Center for Smart Materials, School of Chemical Engineering, Dalian University of Technology, Dalian 116024, China
[2] School of Chemical Engineering, Ocean and Life Sciences, Dalian University of Technology, Panjin 124221, China
* Correspondence: zhaojzh@dlut.edu.cn

How To Cite: Li, W.; Hou, Y.; Zhao, J. Initiation of Radical Photopolymerization with Perylenebisimide Derivatives Having Twisted Molecular Structures as Heavy-Atom-Free Visible Light-Harvesting Efficient Photoinitiators. *PhotoScience Advance* **2025**, *1*(1), 1.

Received:19 June 2025
Revised: 27 July 2025
Accepted: 29 July 2025
Published: 4 August 2025

Abstract: We developed novel visible light-harvesting photoinitiators for radical photopolymerization, based on perylenebisimide (PBI) derivatives having twisted molecular structure and efficient intersystem crossing (ISC). These novel photoinitiators show strong absorption of green light ($\varepsilon = 6.2 \times 10^4$ $M^{-1}cm^{-1}$ at 654 nm), efficient ISC (singlet oxygen quantum yield Φ_Δ is up to 77%), and long-lived triplet excited states (τ_T is up to 334 μs). Fluorescence and triplet state quenching studies show that the triplet excited states of these photoinitiators play a major role for the intermolecular electron transfer with the co-initiator tetrabutylammonium tris(3-chloro-4-methylphenyl)hexylborate (NB) to produce the free radicals, supported by the Stern–Volmer quenching constants for the singlet excited state and triplet excited state, which are 72 M^{-1} and 1.0×10^4 M^{-1}, respectively. Using an alternative co-initiator, diphenyliodonium (DPI), gives much poorer photopolymerization. Interestingly, using two co-initiators of NB and DPI simultaneously in the blends, makes the photopolymerization more efficient and faster, because for the three-component blend, the recombination of electron donor co-initiator NB and electron acceptor co-initiator DPI makes the photoinitiators a photocatalyst, i.e., absorption of one photon will produce two radicals. These results are useful for development of new visible light-absorbing photoinitiators for radical photopolymerization.

Keywords: electron transfer; perylenebisimide; photopolymerization; photoinitiator; triplet state

1. Introduction

Photopolymerization is important for applications in photo-curable resin, photo-curable adhesive, microstructure fabrication and 3D printing, etc. [1−9]. Development of novel photoinitiators is critical for photopolymerization [6−10], as well as for fundamental photochemistry studies [11−13]. Among the various photopolymerization methods, the radical photopolymerization is in particular of interest. Different type of photoinitiators have been developed for radical photopolymerization, such as the Norrish type I initiators [14−16], oxime esters (e.g., OXE-01® or OXE-02,® etc. and new derivatives) [17−19], or the diphenyl(2,4,6-trimethylbenzoyl)phosphine oxide (TPO) [20,21]. Some photoinitiators are used with co-initiator, and the intermolecular electron transfer between the photo excited state of the photoinitiators and the co-initiator will produce reactive free radical to initiate the polymerization of the monomers contain C=C double bonds, such as

Copyright: © 2025 by the authors. This is an open access article under the terms and conditions of the Creative Commons Attribution (CC BY) license (https://creativecommons.org/licenses/by/4.0/).
Publisher's Note: Scilight stays neutral with regard to jurisdictional claims in published maps and institutional affiliations.

acrylates [6−8,22]. Although a great amount of photoinitiators have been developed for this purpose, the road blocking challenge for the development of photopolymerization is the lack of visible light-absorbing photoinitiators, and the in-depth study of the photo-initiating mechanism. Previously most of the photoinitiator absorb in the UV or blue spectral range (this is partially due to the well developed UV or blue LED light source or the mercury lamp light source). Visible light-harvesting photo-initiators are rarely reported.

On the other hand, the photo-initiating mechanisms were rarely studied with transient spectroscopy. For instance, either the singlet excited state or the triplet excited state of the photoinitiators can drive the intermolecular electron transfer with the co-initiators, however, it is rarely clarified whether the singlet or the triplet state plays a major role for the intermolecular electron transfer. From a point of view of photochemistry, the triplet state may be more efficient for driving the intermolecular electron transfer than the singlet excited state because of its much longer lifetime (~μs) than the singlet excited sate (~ns). However, this advantage can be compromised by the lower triplet stale energy than the singlet excited state, which makes the excited state redox potentials less potent to drive the intermolecular electron transfer. Therefore, it is still an open question, i.e., which state plays a major role to drive the intermolecular electron transfer with the co-initiators.

Herein, we used two visible light-absorbing triplet photosensitizer as efficient photoinitiators for radical photopolymerization, and the photoinitiation mechanisms is presented in Scheme 1. Triplet excited state of organic molecules is produced by intersystem crossing (ISC), which is a spin-forbidden process. Various molecular structural motifs have been developed to enhance the ISC in organic molecules, such as by incorporation of heavy atoms in the molecular structure, or using spin converter, or using exciton coupling effect, charge recombination, or using radical enhanced ISC. Recently we and others found that for some chromophores, twisted molecular structure may induce efficient ISC in heavy atom-free compounds. Concerning this strategy, the chromophore of perylenebisimide (PBI) chromophore is in particular of interest because of its strong of electron deficient character. Thus, it is ideal to use these electron deficient photoinitiators with electron donor co-initiators, such as tetrabutylammonium tris(3-chloro-4-methylphenyl)hexylborate (NB), to initiate efficient, visible light radical photopolymerization [22,23].

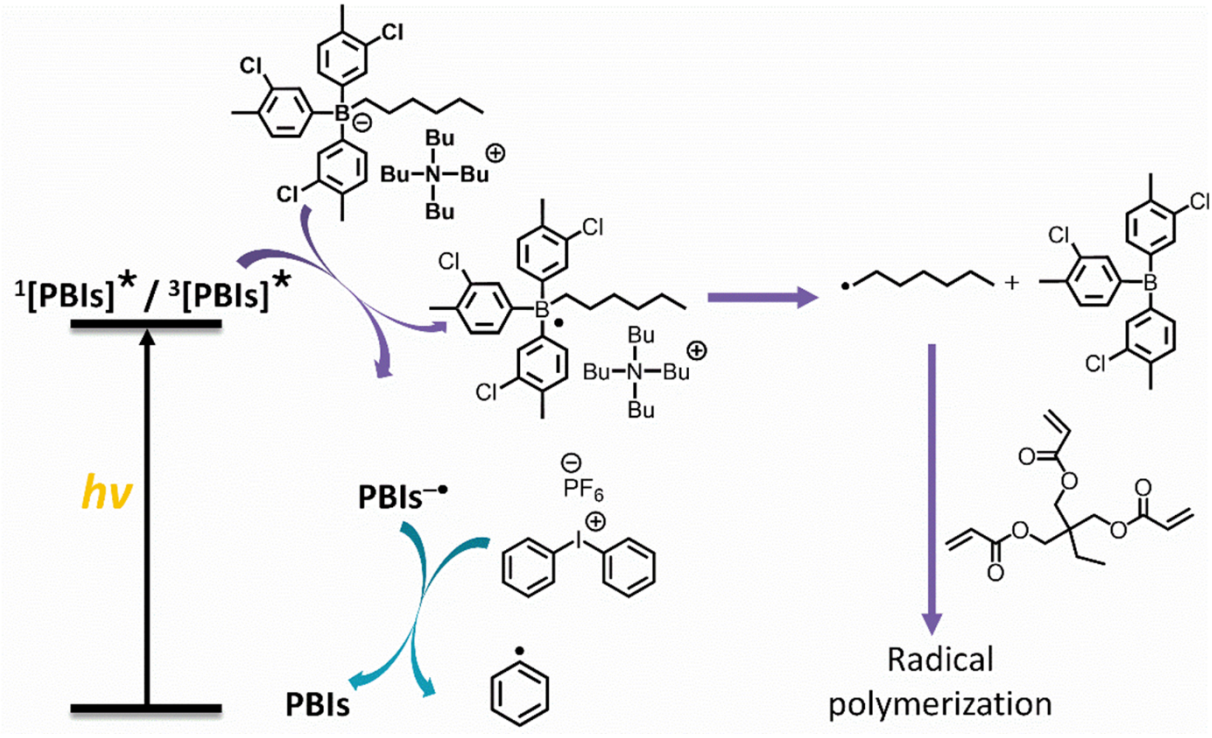

Scheme 1. Photochemical mechanisms for the PBIs/NB/DPI system upon photoexcitation. The three-component system makes the photosensitizer regenerated after producing two reactive radicals, thus it acts as photocatalyst. The asterisks indicate the species are at electronic excited state.

We selected two PBI derivatives which have twisted molecular structures, and show efficient ISC, as well as long-lived triplet excited states (Figure 1) [24,25]. Two typical co-initiators, NB and diphenyliodonium hexafluorophosphate (DPI), were used for photopolymerization studies [24]. The photo initiating mechanism was studied with steady state and transient fluorescence intensity and lifetime quenching, steady state photobleaching,

nanosecond transient absorption spectroscopic methods, as well as time-dependent operando infra-red (IR) spectral monitoring of the double band conversion kinetics and yield of the monomers during the continuous photoirradiation-induced radical photopolymerization processes. The results indicate that the PBI derivatives having twisted molecular structures are efficient visible light-absorbing photoinitiators for radial photopolymerization and simultaneous use of electron donor co-initiator NB and electron acceptor co-initiator DPI may transform the PBI photoinitiators into a photocatalytic species, i.e., two reactive free radicals are produced with one photon, which makes the photopolymerization more efficient [6−8,26−31].

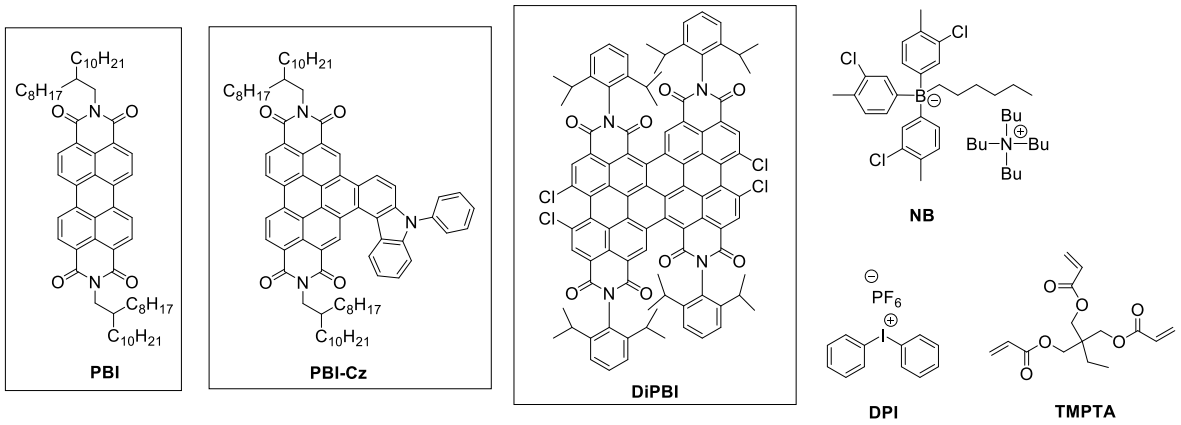

Figure 1. The molecular structures of the photoinitiators (PIs) **PBI**, **PBI-Cz** and **DiPBI**. The molecular structures of the co-initiators (NB and DPI) and the monomer trimethylolpropane triacrylate (TMPTA) are also presented.

2. Experimental Section

2.1. Experimental Methods

The chemicals used in synthesis are analytical pure and were used as received without purification. UV-vis absorption spectra were recorded on a UV-2550 spectrophotometer (Shimadzu Ltd., Kyoto, Japan). Fluorescence emission spectra were recorded with FS5 spectrofluorometer (Edinburgh Instruments Ltd., Livingston, UK).

2.2. Electrochemical Studies

Cyclic voltammetry curves were recorded on a CHI610D electrochemical workstation (Shanghai Chenhua Instruments, China) in N_2 purged DCM solution containing 0.10 M Bu_4NPF_6 as the supporting electrolyte, platinum as the counter electrode; glassy carbon electrode was used as the working electrode; and $Ag/AgNO_3$ (0.1 M in ACN) couple was used as the reference electrode. Ferrocene was used as an internal reference.

2.3. Nanosecond Transient Absorption Spectroscopy

Nanosecond transient absorption spectra were measured with a LP980 laser flash photolysis spectrometer (Edinburgh Instruments Ltd., Livingston, UK), with a Surelite OPO Plus SL I-10 nanosecond laser (Continuum Ltd., Santa Clara, CA, USA). The typical laser pulse energy was 10 mJ per pulse. The transient signals were digitized on a Tektronix TDS 3012B oscilloscope. All samples were purged with N_2 for 15 min before measurements if needed to be measured in a N_2 saturated solution. The data were analyzed with the L900 software.

2.4. Photopolymerization Kinetic Investigations

The photopolymerization kinetic curves were continuously followed by real time FT-IR spectroscopy (Thermo Scientific Nicolet iS20, Waltham, MA, USA), the IR spectra were acquired with 16 scans at 0.25 cm^{-1} resolution. The monomer, co-initiator and PSs were mixed and the mixture was casted evenly on the diamond plate, which was covered with a slide to isolate oxygen. The real-time near-IR spectrum of samples were recorded under irradiation of a 532 nm LED with light intensity of 20 mW/cm^2. The double bonds conversion (DBC) of the blends was calculated by the change of C=C stretching vibrational absorption peak centered at 1640 cm^{-1} and taking C=O peak at 1720–1730 cm^{-1} as internal standard [32,33]. The following Equation (1) was used [33]:

$$\mathrm{DBC}(\%) = \frac{(A_{C=C}/A_{C=O})_0 - (A_{C=C}/A_{C=O})_t}{(A_{C=C}/A_{C=O})_0} \times 100\% \quad (1)$$

where, A_0 is the area before illumination, and A_t is the area after illumination time (t) determined by baseline method.

3. Results and Discussion

3.1. Molecular Structure Design

The electron transfer between the photoexcited photosensitizer and the co-initiators is a diffusion-controlled process, for which the efficiency is dependent on the excited state lifetimes of the photosensitizer, among the other factors. Concerning this aspect, triplet excited state is superior compared to the singlet excited state of the photoinitiators, because of the longer lifetime of the former. Therefore, we selected triplet photosensitizers as photoinitiators (**PBI-Cz** and **DiPBI** in Scheme 1. For the synthesis of **PBI-Cz** and the molecular structure characterization, refer to Supporting Information and Figures S1 and S2). Among the others, heavy-atom-free triplet photosensitizers are in particular of interest, because no heavy atoms are required to incorporated in the molecular structure (such as halogen atoms, Br, I, or precious metal atoms, such as Ir, Ru, Pt, etc.), thus the cost of preparation of such triplet photosensitizers is efficient, and the toxicity is reduced [34,35]. Previously it was reported that the compound **DiPBI** has twisted molecular structure, and efficient ISC was observed (Φ_Δ = 59%) [30]. Notably, the triplet state lifetime was reported as 35 μs [24]. This lifetime is much longer than the lifetimes of singlet excited state (a few ns). Moreover, we also selected another heavy-atom-free triplet photosensitizer (**PBI-Cz**), for which the molecular structure is twisted, and efficient ISC was observed [25]. Previously it was found the triplet state lifetime of **PBI-Cz** is longer (τ_T = 382 μs). Thus, we envision that these heavy-atom-free triplet photosensitizer should be able to be used as efficient photoinitiator for radical photopolymerization.

We selected NB as one co-initiator. NB is a strong electron donor (E_{OX} = +0.43 V, vs. Fc/Fc^+) [36], after transfer an electron to the photoexcited photoinitiator (i.e., **DiPBI** or **PBI-Cz**, which are electron acceptors), the NB molecules will undergo ultrafast decomposition via cleavage of the B–N bond [11], and a highly reactive hexyl free radical is produced, which is able to initiate radical polymerization of the acrylate monomers. We selected a typical monomer trimethylolpropane triacrylate (TMPTA) to demonstrate the photopolymerization (Scheme 1).

Moreover, we also selected another popular co-initiator, diphenyliodonium hexafluorophosphate (DPI), an electron acceptor, for comparison. DPI is a strong electron acceptor, after receiving an electron, a fast decomposition will occur, and a reactive phenyl free radical is produced, which is able to initiate the polymerization of TMPTA. Another rationale to combine the use of NB and DPI simultaneously is that, after electron transfer from NB to PBI photoinitiators, the PBI molecules transform into a radical anion form, which is unable to initiate further radical polymerization. In the presence of DPI (electron acceptor), however, the PBI radical anions is oxidized to the neutral form by DPI, thus it will become active for further photoinitiating. Furthermore, the DPI molecules will produce a phenyl radical to initiate polymerization. Thus, two free radicals are formed with absorption of one photon. All these characters will make the radical photopolymerization more efficient.

3.2. UV-vis Absorption Spectra and Photobleaching

The UV-vis absorption of the compounds was studied previously [24,25]. The major absorption band of **PBI-Cz** is in the range of 400–550 nm, and the molar absorption coefficients is 1.7×10^4 $M^{-1}cm^{-1}$ at the absorption maxima (Figure 2). Notably, this absorption band is much weaker than the unsubstituted PBI. For the **DiPBI**, however, the absorption band is much red-shifted, with an absorption a maximum at 654 nm, with molar absorption coefficients of 6.2×10^4 $M^{-1}cm^{-1}$. The absorption of **DiPBI** is independent on solvent polarity, but **PBI** and **PBI-Cz** are solvent-dependent, probably due to aggregation (Figure S3). The fluorescence of the compounds was studied (Figure S6), it was found the fluorescence intensity and emission maxima are solvent polarity dependent, especially for **PBI-Cz**, indicating the charge transfer character of the emissive S_1 state.

The photophysical property of the compounds is summarized in Table 1. [Generally the photoinitiators are well soluble in ordinary organic solvents]. The data show that **PBI** is highly fluorescent, but the derivatives of **PBI-Cz** and **DiPBI** are weakly fluorescent. The singlet oxygen photosensitizing experiments show that the triplet state yields of **PBI-Cz** and **DiPBI** are high, whereas it is negligible for compound PBI [37].

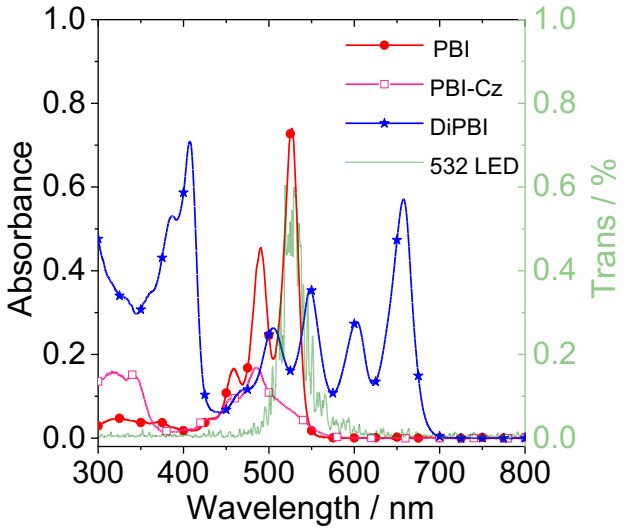

Figure 2. UV-vis absorption spectra of **PBI**, **PBI-Cz** and **DiPBI** in toluene (TOL), c = 1.0 × 10^{-5} M, and the emission spectrum of green LED used in photopolymerization is presented, the emission band is centred at 532 nm, 25 °C.

Table 1. Photophysical parameters of the compounds [a].

Compounds	λ_{abs}/nm [b]	ε [c]	λ_{em}/nm [d]	τ_F/ns [e]	τ_T/μs [f]	Φ_F [g]	Φ_Δ [h]
PBI	526	7.3	537	4.6	126	95.1	[i]
PBI-Cz	485	1.7	611	13.8	334	4.8	39
DiPBI	654	6.2	668	0.8	35	6.9	77

[a] c = 1.0 × 10^{-5} M, in TOL, 20 °C. [b] UV-vis absorption wavelength at the maxima, c = 1.0 × 10^{-5} M. [c] Molar absorption coefficient, ε: 10^4 M^{-1} cm^{-1}. [d] Fluorescence emission wavelength, λ_{ex} = 410 nm. [e] Fluorescence lifetime, λ_{ex} = 405 nm. [f] Triplet lifetime, λ_{ex} = 480 nm. [g] Fluorescence quantum yields determined, in percent. [h] Singlet oxygen ($^1O_2$) quantum yield with 2,6-didiiodoBodipy as standard (Φ_Δ = 87% in DCM), in percent, λ_{ex} = 500 nm. [i] Not observed.

In order to check the possibility of the photo-driven electron transfer between the photoexcited photoinitiators and the co-initiators. The photobleaching of the compounds in TOL with co-initiator added were studied (Figure 3). The UV−vis absorption changes of the **PBI** upon photoirradiation in the presence of electron donor NB was monitored (Figure 3a). With addition of ca. 6 eq of NB, and then 532 nm light exposure, the initial absorption bands of **PBI** at 457 nm, 487 nm and 525 nm decreased slightly, concomitantly, new weak absorption bands centered at 407 nm developed, which are attributed to the photoproduct. However, the absorption peak of the $\mathbf{PBI}^{\cdot-}$ was not observed at 650–950 nm [38]. Similar studies were performed for **PBI-Cz** (Figure 3b), the initial absorption bands of **PBI-Cz** at 426 nm, 455 nm and 485 nm decreased upon photoirradiation in the presence of NB, concomitantly, new absorption bands at 399 nm, 425 nm and 451 nm developed, which are more significantly than that of **PBI**. For **DiPBI** (Figure 3c), moreover, the new absorption bands also appeared in the near-infrared band at 720 nm and 870 nm. In the absence of NB, however, photo-irradiations of the photoinitiators does not lead to any change of the UV-vis absorption of the photo-initiators (Figure S4). When both NB and DPI are present in the solution electron donors, the initial absorption bands of **DiPBI** decreased and new absorption bands were generated (Figure S5b), whereas **PBI-Cz** remains unchanged (Figure S5a). The photography of the solutions upon photoirradiation are presented (Figure 3d–f). These results infer that photo-driven intermolecular electron transfer between the photoexcited initiator and the co-initiator NB occurs, and these systems may be used for radical photopolymerization. Moreover, the results also show that **PBI-Cz** and **DiPBI** should be more efficient photoinitiators than **PBI**. These anticipations are confirmed by the photopolymerization studies (see later section).

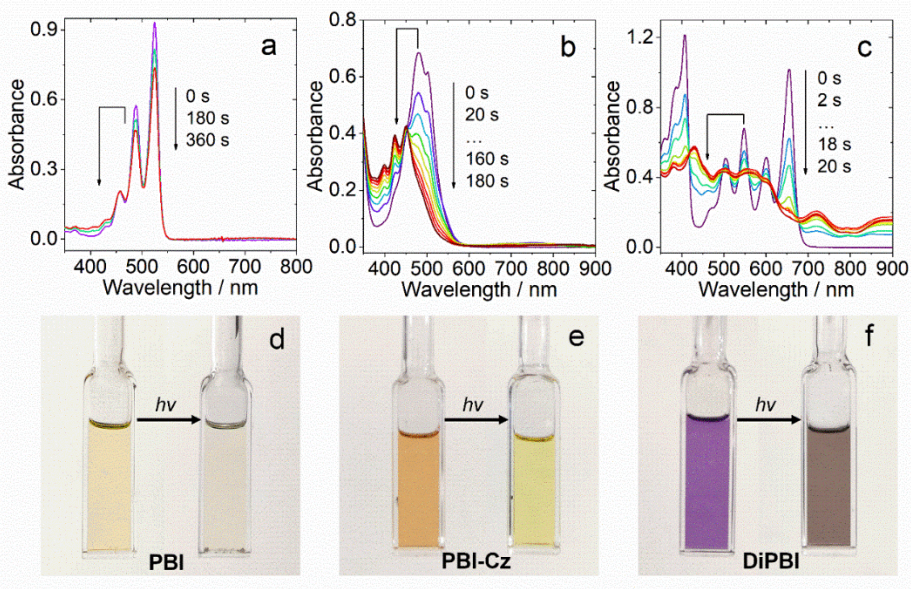

Figure 3. UV-vis absorption spectra of (**a**) **PBI** (1.0×10^{-5} M), (**b**) **PBI-Cz** (5.0×10^{-5} M) and (**c**) **DiPBI** (1.5×10^{-5} M) upon exposure to 532 nm LED in the presence of 6 eq. NB in deaerated dichloromethane (DCM). Photographs showing the reversible color change of the (**d**) **PBI**/NB, (**e**) **PBI-Cz**/NB and (**f**) **DiPBI**/NB mixed solution upon sequential photoirradiation, c[NB] = 1.0×10^{-3} M, the light power density is 5 mW/cm^2, 25 °C.

3.3. Electrochemical Studies

In order to study the thermodynamics of the intermolecular electron transfer between the photoexcited photoinitiator and the co-initiators. The electrochemical properties of compounds were studied by cyclic voltammograms (Figure 4). For **PBI**, two reversible reduction waves at −1.08 V and −1.28 V (vs. Fc/Fc$^+$) were observed. For **PBI-Cz**, two reversible reduction potential of −1.13 V and –1.39 V can be observed. One irreversible oxidation potential wave at +1.04 V was observed. For **DiPBI**, the reduction waves were observed at −0.52 V and −0.81 V, respectively. And two reduction waves at −1.50 V and −1.63 V were observed. These results indicate that **DiPBI** is a stronger electron acceptor than unsubstituted PBI. This is beneficial for use of these photoinitiators with the electron donor co-initiators of NB.

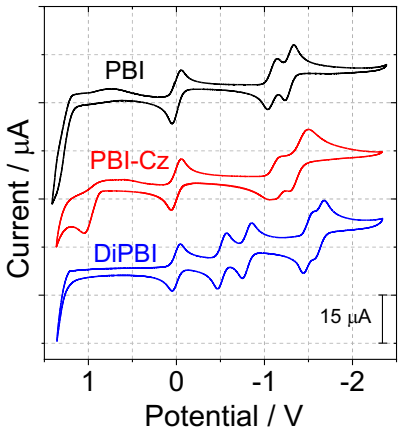

Figure 4. Cyclic voltammograms of **PBI**, **PBI-Cz** and **DiPBI** in deaerated DCM containing 0.10 M Bu_4NPF_6 as supporting electrode and with $Ag/AgNO_3$ reference electrode. Scan rate: 100 mV/s. c = 1.0×10^{-3} M. Ferrocene (Fc) was used as internal reference, 20 °C.

The free energy changes for the intermolecular electron transfer process were calculated with the (eq 2). The data are collected in Table 2.

$$\Delta G_{ET} = e[E_{OX} - E_{RED}] - E_{00} - C \quad (2)$$

ΔG_{ET} is the Gibbs free energy change of the electron transfer, E_{ox}, E_{RED}, E_{00} and C are the oxidation potentials of the electron donor, the reduction potential of the electron acceptor, the excited state energy and the Coulomb term for the initially formed ion pair, respectively. C is neglected as usually done in polar solvents for intermolecular electron transfer.

The data are summarized in Table 2. The data show that the electron transfer between the singlet excited state of the photo-initiators and the co-initiator is highly exothermic, i.e., the electron transfer is thermodynamically allowed. However, this advantage will be decremented by the short singlet excited state lifetimes. On the other hand, the electron transfer for the triplet excited state is slightly endothermic, i.e., the electron transfer between the triplet excited state and the co-initiator NB is slightly thermodynamically forbidden. However, our later studies show that the triplet state plays a major role for initiating the radical polymerization. Thus, the determination errors for the photophysical parameters may contribute to this contradictory prediction.

Table 2. Redox Potential, Gibbs Free Energy Changes between the photosensitizer and co-initiator for compounds [a].

Compounds	E_{RED}/V [a]	E_{OX}/V [b]	E_{00}/V [c]	E_T/V [d]	ΔG_{ET} (NB)/eV	ΔG_{ET} (DPI)/eV [f]
PBI	−1.08	[h]	2.25	1.24	−0.74 [e]/+0.27 [f]	[h]
PBI-Cz	−1.13	+1.04	2.21	1.32	−0.65 [e]/+0.24 [f]	−0.10[e]/+0.79[f]
DiPBI	−0.52	[h]	1.92	1.11 [g]	−0.97 [e]/−0.16 [f]	[g]

[a] Reduction potential of –1.07 V is used for DPI; [b] Oxidation potential of +0.43 V is used for NB; [c] $E_{00} = 1240/\lambda$. E_{00} is the singlet excited state energy, λ is the wavelength of the on-set of the luminescence of the compound; [d] E_T for the first triplet excited state energy, calculated by DFT; [e] ΔG_{ET} for the singlet excited state, calculated by Equation (2); [f] ΔG_{ET} for the first triplet excited state, calculated by Equation (2); [g] literature value; [h] Not observed.

3.4. Quenching of the Fluorescence and Triplet States of the Photosensitizers by Co-Initiator: Study of the Photoinitiating Mechanism

In order to study the photo-initiating mechanism, the variation of the fluorescence spectra of **PBI**, **PBI-Cz** and **DiPBI** in the presence of NB were investigated (Figure 5). With incremental addition of NB in the TOL solution, the fluorescence of **PBI-Cz** is quenched (Figure 5a) and a weak band was observed at 520 nm. Similar quenching effect was observed in DCM solution (Figure S8). In contrast, the fluorescence intensity of **PBI** and **DiPBI** has no change upon incremental addition of NB (Figures S7 and S9. Supporting Information). The lack of fluorescence variation of **DiPBI** may be attributed to the short fluorescence lifetimes (0.8 ns, Table 1).

Base on the fluorescence quenching with NB as quencher, and Stern–Volmer equation (Equation (3)), the quenching was quantitatively characterized (Table 3). The quenching of the fluorescence lifetime of **PBI-Cz** was studied by the Stern–Volmer equation (Equation (3), Figure 6), and a Stern–Volmer quenching constant of 72 M^{-1} was obtained. For **PBI** and **DiPBI**, however, the quenching constants are negligible.

$$\tau_0/\tau_t = 1 + K_{SV}[NB] \quad (3)$$

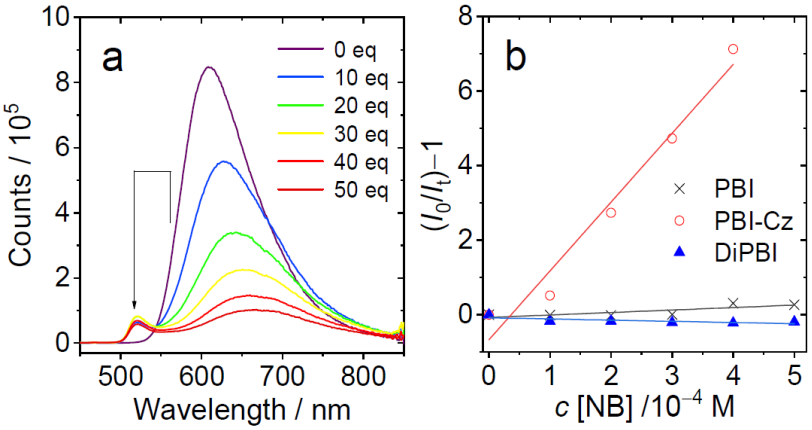

Figure 5. Fluorescence quenching spectra of (**a**) **PBI-Cz** under air atmospheres in TOL upon increamental of NB, λ_{ex} = 410 nm, $c = 5.0 \times 10^{-5}$ M. (**b**) The corresponding Stern–Volmer plot for compounds.

Table 3. K_{SV} and k_q of the Compounds [a].

Compounds	Fluorescence [b]	K_{SV}^F [c]	K_{SV}^T [d]	k_q^F [c]	k_q^T [d]
PBI	0.1×10^4	1.2	[e]	2.6×10^8	[e]
PBI-Cz	1.8×10^4	72	1.0×10^4	52×10^8	0.3×10^4
DiPBI	[e]	[e]	3.4×10^4	[e]	9.7×10^4

[a] Stern–Volmer quenching constants, K_{SV}: M^{-1}, bimolecular rate constant for collisional quenching, k_q: $M^{-1} \cdot s^{-1}$, NB as a quencher. [b] Obtained by fluorescence intensity quenching under air atmosphere. [c] Fitted by fluorescence lifetime quenching under air atmosphere. [d] Obtained by triplet state lifetime quenching under N_2. [e] Not observed.

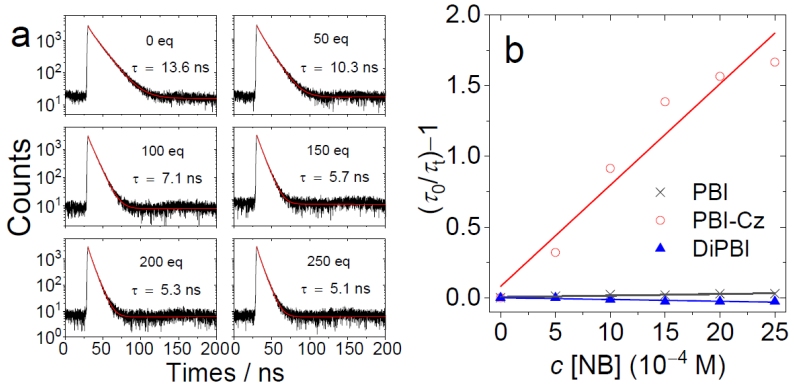

Figure 6. (**a**) Fluorescence decay traces of **PBI-Cz** at 405 nm, in the presence of NB; (**b**) the corresponding Stern–Volmer plot for compounds, $c = 1.0 \times 10^{-5}$ M in DCM, $\lambda_{ex} = 405$ nm.

We also used the variation of the fluorescence lifetimes of the compounds in the presence of NB to study the quenching. With addition of the co-initiator NB, significant quenching of fluorescence lifetime of **PBI-Cz** was observed (Figure 6), but the addition of DPI did not lead to a significant shorting of the fluorescence lifetime. However, for the fluorescence lifetime of **PBI** and **DiPBI**, with either NB or DPI is added, it is virtually not quenched (Figures S7, S9 and S10). Note this trend is in agreement with the fluorescence intensity quenching studies.

In order to study the quenching of the triplet excited states of the photo-initiators by the co-initiator NB, the nanosecond transient absorption (ns-TA) spectra of the compounds were studied. Firstly, the ns-TA spectra of the photo-initiators alone were recorded (Figure 7). An excited state absorption (ESA) band at 536 nm was observed, as well as a weak ground state bleaching (GSB) band centered at 470 nm. Note the ESA band and the GSB band may overlap with each other, and both bands are distorted. The triplet state lifetime of **PBI-Cz** was determined as 334 μs (Inset of Figure 7a), which is close to the previous report of the triplet state lifetimes (τ_T = 382 μs) [25]. Note the triplet state lifetime is highly dependent on the experimental conditions, such as concentration of the compounds, the energy of the laser pulse, and the trace oxygen in the solution. The ns-TA spectra of **DiPBI** were also studied (Figure 7b), as compared to **PBI-Cz**, red-shifted GSB bond centered at 650 nm was observed. The triplet state lifetime of **DiPBI** was determined as 35 μs, the same to the previous report [25].

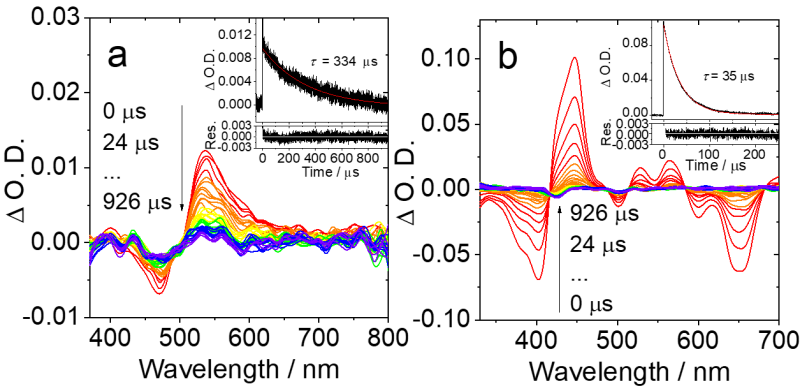

Figure 7. Nanosecond transient absorption spectra of (**a**) **PBI-Cz** and (**b**) **DiPBI** in deaerated DCM. Insets are the corresponding decay traces monitored for **PBI-Cz** at 550 nm and **DiPBI** at 455 nm in deaerated DCM. $c = 1.0 \times 10^{-5}$ M, $\lambda_{ex} = 480$ nm, 25 °C.

The quenching of the triplet state of **PBI-Cz** and **DiPBI** by NB as electron donor was studied by the construction of Stern–Volmer plot (Figure 8). In the presence of higher concentration of NB, the triplet state lifetime of **PBI-Cz** is shortened (Figure 8a). For instance, the triplet state lifetime of 334 μs in the absence NB, was shortened to 177 μs in the presence of 12 equivalent of NB, and further shortened to 103 μs in the presence of 24 equivalent of NB. Similar quenching effect was observed for **DiPBI**. Stern–Volmer quenching constants of 1.0 × 10^4 M^{-1} and 3.4 × 10^4 M^{-1} were determined for **PBI-Cz** and **DiPBI**, respectively. These values indicate the intermolecular electron transfer between the triplet excited states of the photo-initiators and the co-initiators.

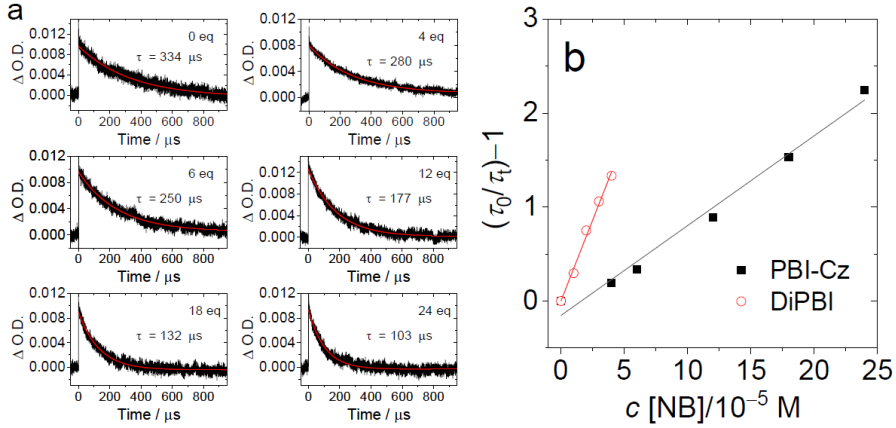

Figure 8. (**a**) The decay traces of **PBI-Cz** (1.0 × 10^{-5} M) at 550 nm in deaerated DCM upon incremental addition of NB, (**b**) the corresponding Stern–Volmer plot for compounds, c = 1.0 × 10^{-5} M, λ_{ex} = 480 nm, 25 °C.

3.4. Photopolymerization Investigations

Next, we carried out radical photopolymerization with the photoinitiators in different blends compositions (Figure 9). First, the mixture of photoinitiators and the monomer TMPTA were photoirradiated in the absence of co-initiators (top row in Figure 9. 532 nm LED was used). Note we select TMPTA not for low toxicity, it is for the reason that three C=C double bonds are present and the cross linking will make the solidification of the blend feasible. For application in dental clinics, acrylates monomers with low toxicity should be used. The blends did not solidify even upon 15 min exposure to green LED light. Interestingly, with addition of NB into the blends, solidification of the blends was observed upon photoirradiation. For **PBI**, 4 min. of photoirradiation is required for the radical polymerization. For **PBI-Cz** and **DiPBI**, however, much shorter photoirradiation time is required, for **PBI-Cz**, 15 s of photoirradiation is required, for **DiPBI**, 7 s photoirradiation is sufficient. Each photopolymerization experiment was repeated for three times. These results indicates that **PBI-Cz** and **DiPBI** are promising efficient photoinitiators for radical photopolymerization. Note the photopolymerization experiments were carried out under N_2 atmosphere because it is known the O_2 molecules will retard the radical photopolymerization. Producing of radicals in the photoinitiating system was confirmed by EPR spectral study in the presence of radical scavenger *N*-*tert*-butyl-*α*-phenylnitrone (PBN. Figure S11).

We also studied the radical photopolymerization with DPI as co-initiator (DPI is an electron acceptor, the third row from the top). For **PBI**, no solidification of the blend was observed even for 15 min. of photoirradiation. For **PBI-Cz** and **DiPBI**, 10 min of photoirradiation was required for solidification of the blend. These results indicate DPI is a poor co-initiator to be used with the current photoinitiators. The possible reason is that the photoinitiators studied herein are electron acceptors, therefore the photoinitiator/DPI is not good combination to initiate radical photopolymerization. In all these photopolymerizations, the color of the blend is persistent, unless a photobleaching experiment is carried out. Photobleaching is important for applications such as in dental clinics [39,40].

Considering the reaction mechanism of photoinitiator/NB, after photo-induced electron transfer between the photoexcited photoinitiators and the co-initiator NB, the photoinitiators were reduced to the radical anions, these species are inactive for further initiation of radical photopolymerization, and photoexcitation of these radical anions will not drive electron transfer with NB (electron donor), because the photoexcited radical anions of the photo-initiators are strong electron donor. Therefore, we envision that these ‘dead’ radical anions can be re-activated if they are oxidized to its neutral form, by an electron acceptor type of co-initiator. In this case, one photon can produce at least two reactive radicals to initiate radical photopolymerization. Following thess rationales, we added DPI to the blends, and we found the solidification of the blends photoinitiator/NB/TMPTA is achieved

with much shorter photoirradiation time. For instance, only 76 s is required for solidification of the blend with both NB and DPI were used (**PBI** as the photoinitiator), in comparison, 4 min is required for the solidification with only NB as the co-initiator. Similarly, the solidification for the blends with **PBI-Cz** and **DiPBI** become much shorter with both NB and DPI added, only 5 s and 3 s of photoirradiation are required, respectively. These results indicate that the three components photopolymerization blends are efficient, and a catalytic cycle is realized with use of two co-initiators, one is electron donor (NB), and another is an electron acceptor (to oxidize the radical) anion of the photo-initiators to regenerate it to initiate radical photopolymerizations [6−8,27−31,41].

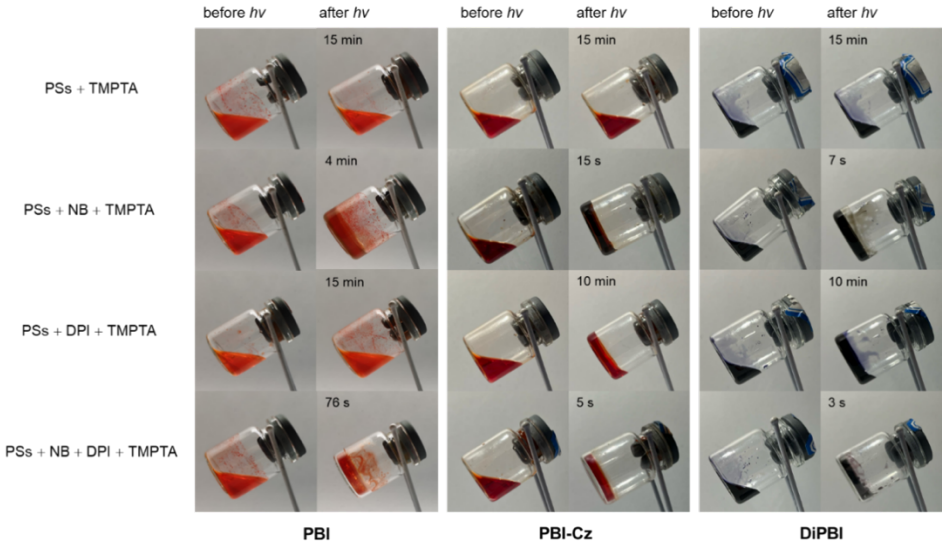

Figure 9. The photopolymerization of TMPTA under N_2 before and after irradiation using 20 mW/cm^2 upon 532 nm LED in the presence of **PBI, PBI-Cz**, **DiPBI** and co-initiator. For the vials from top row to the bottom row, the components of the blends are photosensitizer (0.2%), photosensitizer/NB (0.2 w%/1.0 w%), photosensitizer/DPI (0.2 w%/1.0 w%) and photosensitizer/NB/DPI (0.2 w%/1.0 w%/1.0 w%), respectively. The percentage of each component is relative to the TMPTA monomer and each sample contains 0.1 mL DCM.

In order to more precisely study the radical photopolymerization of the different blends, we monitored the photopolymerization kinetics by following the conversion of the double bonds in the monomers, by using the Infra-red (IR) spectrometer to collect series. The IR spectral study show that **PBI** alone (without any co-initiators) did not induce any radical photopolymerization (Figure 10). No photopolymerization was observed for blend with DPI added as co-initiator. Photopolymerization was observed with NB added as co-initiator, however, an induction period is required, which is possibly due to the consumption of the O_2 in the blend. This effect is typical for radical photopolymerizations, which can be quenched by O_2 molecules [29,42−45]. The conversion rate of the double bonds is not high, ca. 30% in 75 s. With both NB and DPI added as co-initiator, the blend gives a much faster polymerization, the induction period is becomes shorter, and the conversion ratio of the double bonds of the blend is up to 60%.

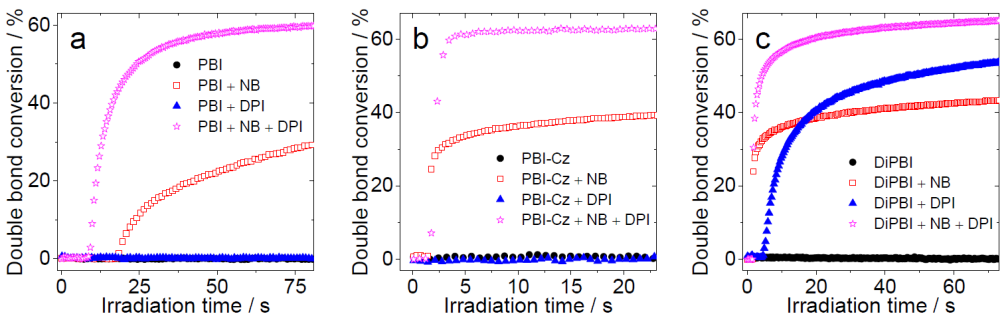

Figure 10. Photopolymerization profiles in the presence of (**a**) **PBI**, (**b**) **PBI-Cz** and (**c**) **DiPBI**. Photoinitiator (0.2%), photoinitiator/NB (0.2 w%/1.0 w%), photoinitiator /DPI (0.2 w%/1.0 w%) and photoinitiator /NB/DPI (0.2 w%/1.0 w%/1.0 w%). The percentage of each component is relative to the monomer and each sample contains 0.1 mL DCM, TMPTA as the monomer. The light source at 532 nm with 20 mW/cm^2 irradiation intensity. The irradiation starts at t = 2 s.

Similar trend was observed with **PBI-Cz** as photoinitiator (Figure 9b). As compared to **PBI** as photo-initiator, **PBI-Cz**/NB shows much shorter induction period, and the photopolymerization is much faster. Higher conversion yield of the double bond of the monomer was observed for **PBI-Cz**/NB/DPI blend. Even better performance was observed for **DiPBI** as photoinitiator, in this case, photopolymerization was observed for the blend of **DiPBI**/DPI. Overall, these results indicate that the PBI derivatives are promising photoinitiators, expecially **PBI-Cz** and **DiPBI**, and using paired co-initiators of NB and DPI makes the system more efficient for radical photopolymerization.

The radical photopolymerization mechanism is summarized in Scheme 1. Upon photoexcitation of the photoinitiators, firstly the singlet excited state is populated, then for **PBI-Cz** and **DiPBI**, triplet excited state was produced via efficient ISC. Note the lifetime of the tripled exited state is much longer than that of singlet excited stale, although the excited stale reduction potential of the triplet excited state is compromised as compared to that of the singlet excited state. After abstract one electron from NB, the photoinitiators are reduced to radical anion, this is a 'dead' species which is unable to initiate further photopolymerization. Upon lose an electron, NB gives a highly reactive hexyl radical to initiate radical polymerization the monomer.

Upon addition of extra co-initiator DPI in the blend, however the otherwise 'dead' species of the photo-initiators radical anion is oxidized to the neutral form, which can photoexcited and initiate further electron transfer with NB. At the same time, the reduced DPI will give phenyl radical, which also initiate the polymerization of the monomers. Thus, the regeneration of the neutral PBI photoinitiators by using the secondary DPI co-initiator transform the photo initiaton to photocatalytic initiators, make the radical polymerization blends more efficient [6−8,26,28].

4. Conclusions

In summary, we developed perylenebisimide (PBI) derivatives with twisted molecular structure and efficient intersystem crossing (ISC), as novel photoinitiators for free radical photopolymerization. These novel photoinitiators show strong absorption of green light (for **PBI-Cz**, $\varepsilon = 1.7 \times 10^4$ $M^{-1}cm^{-1}$ at 485 nm) or red light (for **DiPBI**, $\varepsilon = 6.2 \times 10^4$ $M^{-1}cm^{-1}$ at 654 nm), efficient ISC (singlet oxygen quantum yield $\Phi_\Delta = 39\%$ for **PBI-Cz** and $\Phi_\Delta = 77\%$ for **DiPBI**), and long-lived triplet excited states ($\tau_T = 334$ μs for **PBI-Cz**, and $\tau_T = 35$ μs for **DiPBI**). Fluorescence and triplet state quenching studies show that the triplet excited states of these photoinitiators play a major role for the intermolecular electron transfer with the co-initiator of tetrabutylammonium tris(3-chloro-4-methylphenyl)hexylborate (NB). For instance, the Stern−Volmer quenching constants of **PBI-Cz** singlet excited state and triplet excited state are 72 M^{-1} and 1.0×10^4 M^{-1}, respectively, with NB as quencher (electron donor). Upon electron transfer, the oxidized NB decompose rapidly, to give a highly reactive hexyl radicals, which initiate the radical polymerization of the monomer trimethylolpropane triacrylate (TMPTA). This envisions are confirmed by the photoirradiation induced solidification of different blends. Using an alternative co-initiator, diphenyliodonium (DPI), gives much poorer photopolymerization. Interestingly, using two co-initiators of NB and DPI simultaneously in the blend, makes the photopolymerization more efficient and faster, because the otherwise unreactive radical anion of the photoinitiator (formed by the intermolecular electron transfer) is oxidized to the neutral form, which is able to be photoexcited again and initial the subsequent electron transfer with NB. At the same time, the reduced DPI will produce phenyl radical, which is known to be able to initiate polymerization of the monomer. Thus, the three-component blend, the recombination of electron donor co-initiator NB and electron acceptor co-initiator DPI makes the photo-initiators a photocatalyst, i.e., absorption of one photon will produce two radicals, which makes the radical photopolymerization more efficient, than using only one co-initiator of either NB or DPI. All these results are corroborated by the continuously monitoring the double bond conversion ration of the monomers by using the IR spectrometer. These results are useful for development of new visible light-absorbing photoinitiators for radical photopolymerization.

Supplementary Materials

NMR and HR-MS spectra, steady state UV-vis absorption and luminescence spectra and nanosecond transient absorption spectra details. The Supporting information can be downloaded at: https://media.sciltp.com/articles/others/250804114039498 8/SupportingInformation-Revised.pdf.

Author Contributions

J.Z. conceived the research, acquired the funding and write the manuscript; W.L. synthesized the compounds, performed the steady state and the time-resolved spectral studies, as well as the electrochemistry, photopolymerization and performed parts of the data analysis; Y.H. did part of data analysis and writing of the manuscript. All authors provided comments on writing and modification of the manuscript. All authors have read and agreed to the published version of the manuscript.

Funding

This work was supported by NSFC (22473021 and U2001222), the National Key Research and Development Program of China (2023YFE0197600), the State Key Laboratory of Fine Chemicals, the Research and Innovation Team Project of Dalian University of Technology (DUT2022TB10), the Fundamental Research Funds for the Central Universities (DUT22LAB610).

Institutional Review Board Statement

Not applicable.

Informed Consent Statement

Not applicable.

Data Availability Statement

All the research data associated to this manuscript have been included as a part of the Supplementary Information.

Conflicts of Interest

The authors declare no competing financial interest.

References

1. Topa, M.; Ortyl, J. Moving Towards a Finer Way of Light-Cured Resin-Based Restorative Dental Materials: Recent Advances in Photoinitiating Systems Based on Iodonium Salts. *Materials* **2020**, *13*, 4093.
2. Breloy, L.; Losantos, R.; Sampedro, D.; et al. Allyl Amino-Thioxanthone Derivatives as Highly Efficient Visible Light H-Donors and Co-Polymerizable Photoinitiators. *Poly. Chem.* **2020**, *11*, 4297–4312.
3. Wang, Q.; Popov, S.; Feilen, A.; et al. Rational Selection of Cyanines to Generate Conjugate Acid and Free Radicals for Photopolymerization Upon Exposure at 860 nm. *Angew. Chem. Int. Ed.* **2021**, *60*, 26855–26865.
4. Xue, T.; Huang, B.; Li, Y.; et al. Enone Dyes as Visible Photoinitiator in Radical Polymerization: The Influence of Peripheral *N*-Alkylated (Hetero)Aromatic Amine Group. *J. Photochem. Photobio. A Chem.* **2021**, *419*, 113449.
5. Xu, C.; Gong, S.; Wu, X.; et al. High-Efficient Carbazole-Based Photo-Bleachable Dyes as Free Radical Initiators for Visible Light Polymerization. *Dyes. Pigment.* **2022**, *198*, 110039.
6. Balcerak, A.; Kabatc, J. Recent Progress in the Development of Highly Active Dyeing Photoinitiators Based on 1,3-Bis(P-Substituted Phenylamino)Squaraines for Radical Polymerization of Acrylates. *Poly. Chem.* **2022**, *13*, 1787–1812.
7. Zhao, X.; Xu, H.; Liu, Z.-T.; et al. Designable Polypyrrole Pattern in Hydrogel Achieved by Photo-controllable Concentration of Fe^{3+} Initiator. *Smart Mol.* **2024**, *2*, e20240015.
8. Wang, S.-Y.; Pan, Y.-H.; Qu, Y.-C.; et al. Activatable Theranostic Prodrug Scaffold with Tunable Drug Release Rate for Sequential Photodynamic and Chemotherapy. *Smart Mol.* **2024**, *2*, 20230024.
9. Dumur, F. Recent Advances in Monocomponent Visible Light Photoinitiating Systems Based on Sulfonium Salts. *Polymers* **2023**, *15*, 4202.
10. Wloka, T.; Gottschaldt, M.; Schubert, U.S. From Light to Structure: Photo Initiators for Radical Two-Photon Polymerization. *Chem. Eur. J.* **2022**, *28*, e202104191.
11. Chatterjee, S.; Davis, P.D.; Gottschalk, P.; et al. Photochemistry of Carbocyanine Alkyltriphenylborate Salts: Intra-Ion-Pair Electron Transfer and the Chemistry of Boranyl Radicals. *J. Am. Chem. Soc.* **1990**, *112*, 6329–6338.
12. Davis, H.F.; Lee, Y.T. Photodissociation Dynamics of Clo Radicals at 248 Nm. *J. Phys. Chem.* **1996**, *100*, 30–34.
13. Fast, D.E.; Lauer, A.; Menzel, J.P.; et al. Wavelength-Dependent Photochemistry of Oxime Ester Photoinitiators. *Macromolecules* **2017**, *50*, 1815–1823.
14. Ma, X.; Gu, R.; Yu, L.; et al. Conjugated Phenothiazine Oxime Esters as Free Radical Photoinitiators. *Poly. Chem.* **2017**, *8*, 6134–6142.
15. He, X.; Gao, Y.; Nie, J.; et al. Methyl Benzoylformate Derivative Norrish Type I Photoinitiators for Deep-Layer Photocuring under near-UV or Visible Led. *Macromolecules* **2021**, *54*, 3854–3864.
16. Dumur, F. Recent Advances on Visible Light Triphenylamine-Based Photoinitiators of Polymerization. *Eur. Poly. J.* **2022**, *166*, 111036.
17. Wang, W.; Jin, M.; Pan, H.; et al. Remote Effect of Substituents on the Properties of Phenyl Thienyl Thioether-Based Oxime Esters as Led-Sensitive Photoinitiators. *Dyes. Pigment.* **2021**, *192*, 109435.

18. Liu, S.; Graff, B.; Xiao, P.; et al. Nitro-Carbazole Based Oxime Esters as Dual Photo/Thermal Initiators for 3d Printing and Composite Preparation. *Macromol. Rapid Commun.* **2021**, *42*, 2100207.
19. Hammoud, F.; Hijazi, A.; Schmitt, M.; et al. A Review on Recently Proposed Oxime Ester Photoinitiators. *Eur. Poly. J.* **2023**, *188*, 111901.
20. Xie, C.; Wang, Z.; Liu, Y.; et al. A Novel Acyl Phosphine Compound as Difunctional Photoinitiator for Free Radical Polymerization. *Progress Org. Coat.* **2019**, *135*, 34–40.
21. Dietlin, C.; Trinh, T.T.; Schweizer, S.; et al. New Phosphine Oxides as High Performance near- UV Type I Photoinitiators of Radical Polymerization. *Macromolecules* **2020**, *25*, 1671.
22. Giacoletto, N.; Ibrahim-Ouali, M.; Dumur, F. Recent Advances on Squaraine-Based Photoinitiators of Polymerization. *Eur. Poly. J.* **2021**, *150*, 110427.
23. Jędrzejewska, B.; Wejnerowska, G. Highly Effective Sensitizers Based on Merocyanine Dyes for Visible Light Initiated Radical Polymerization. *Polymers* **2020**, *12*, 1242.
24. Wu, Y.; Zhen, Y.; Ma, Y.; et al. Exceptional Intersystem Crossing in Di(Perylene Bisimide)S: A Structural Platform toward Photosensitizers for Singlet Oxygen Generation. *J. Phys. Chem. Lett.* **2010**, *1*, 2499–2502.
25. Mahmood, Z.; Sukhanov, A.A.; Rehmat, N.; et al. Intersystem Crossing and Triplet-State Property of Anthryl- and Carbazole-[1,12]Fused Perylenebisimide Derivatives with a Twisted π-Conjugation Framework. *J. Phys. Chem. B* **2021**, *125*, 9317–9332.
26. Bi, Y.; Neckers, D.C. A Visible Light Initiating System for Free Radical Promoted Cationic Polymerization. *Macromolecules* **1994**, *27*, 3683–3693.
27. Toba, Y.; Usui, Y.; Alam, M.M.; et al. Onium Butyltriphenylborates as Donor−Acceptor Initiators for Sensitized Photopolymerizations of Vinyl Monomer. *Macromolecules* **1998**, *31*, 6022–6029.
28. Toba, Y.; Usui, Y.; Konishi, T.; et al. Visible Light Polymerization of Acrylate Using Dialkylphenacylsulfonium Butyltriphenylborate Initiators: Effect of the Reduction Potential of the Sulfonium Cation on the Polymerization. *Macromolecules* **1999**, *32*, 6545–6551.
29. Jędrzejewska, B.; Pietrzak, M.; Rafiński, Z. Phenyltrialkylborates as Co-Initiators with Cyanine Dyes in Visible Light Polymerization of Acrylates. *Polymer* **2011**, *52*, 2110–2119.
30. Zivic, N.; Bouzrati-Zerelli, M.; Kermagoret, A.; et al. Photocatalysts in Polymerization Reactions. *ChemCatChem* **2016**, *8*, 1617–1631.
31. Sun, K.; Xiao, P.; Dumur, F.; et al. Organic Dye-Based Photoinitiating Systems for Visible-Light-Induced Photopolymerization. *J. Poly. Sci.* **2021**, *59*, 1338–1389.
32. Gan, J.; Hanna, G.; Minhee, J.; et al. Influence of Postwashing Process on the Elution of Residual Monomers, Degree of Conversion, and Mechanical Properties of a 3D Printed Crown and Bridge Materials. *Dent. Mater.* **2022**, *38*, 1812–1825.
33. Yuri, R.; Egor, P.; Aliya, M.; et al. Investigation of the Light Intensity and Temperature Influences on Double Bond Conversion in Resins for Vat Photopolymerization via Fourier Transform Infrared Spectroscopy. *Macromol. Chem. Phys.* **2025**, *226*, 2400398.
34. Enkhjargal, B.; Hanna, G.; Na-Kyung, H.; et al. Influence of Different Postcuring Parameters on Mechanical Properties and Biocompatibility of 3D Printed Crown and Bridge Resin for Temporary Restorations. *Mech. Behav. Biomed. Mater*. **2022**, *128*, 105127.
35. Yuri, R.; Valery, K.; Dmitriy, B.; et al. Comprehensive Investigation of Phosphine Oxide Photoinitiators for Vat Photopolymerization. *Prog. Addit. Manuf.* **2025**, 1–14.
36. Niederst, L.; Allonas, X.; Ley, C.; et al. Introducing a New Electron Acceptor for the Implementation of Photocyclic Initiating System for Radical Photopolymerization. *J. Photochem. Photobio. A Chem.* **2025**, *462*, 116255.
37. Goodson, F.S.; Panda, D.K.; Ray, S.; et al. Tunable Electronic Interactions between Anions and Perylenediimide. *Org. Biomol. Chem.* **2013**, *11*, 4797–4803.
38. Heitmüller, J.; Fröhlich, R.; Renner, R.; et al. Intersystem Crossing of Perylene Bisimide Neutral, Radical Anion, and Dianion Derivatives Compared Via Ultrafast Spectroelectrochemistry. *Phys. Chem. Chem. Phys.* **2023**, *25*, 17214–17229.
39. Dohyun, K.; Ji-Suk, S.; Dasun, L.; et al. Effects of Post-Curing Time on the Mechanical and Color Properties of Three-Dimensional Printed Crown and Bridge Materials. *Polymers* **2020**, *12*, 2762.
40. Filimonova, E.; Lozovaya, A.; Prosyankin, E.; et al. Thermal Treatment Influence on Optical Properties of 3D Printed Objects by Vat Photopolymerization. *Prog. Addit. Manuf.* **2025**, *10*, 2703–2713.
41. Dumur, F. Recent Advances on Visible Light Bodipys and Related Difluoroborane Structures-Based Photoinitiating Systems. *Eur. Poly. J.* **2023**, *196*, 112241.
42. Kabatc, J.; Pączkowski, J. One Photon-Two Free Radical Photoinitiating Systems. Novel Approach to the Preparation of Dissociative, Multicomponent, Electron-Transfer Photoinitiators for Free Radical Polymerization. *Macromolecules* **2005**, *38*, 9985–9992.

43. Kabatc, J.; Jędrzejewska, B.; Pączkowski, J. Asymmetric Cyanine Dyes as Fluorescence Probes and Visible-Light Photoinitiators of Free-Radical Polymerization Processes. *J. Appl. Poly. Sci.* **2006**, *99*, 207–217.
44. Kostrzewska, K.; Ortyl, J.; Dobosz, R.; et al. Squarylium Dye and Onium Salts as Highly Sensitive Photoradical Generators for Blue Light. *Poly. Chem.* **2017**, *8*, 3464–3474.
45. Bouzrati-Zerelli, M.; Kirschner, J.; Fik, C.P.; et al. Silyl Glyoxylates as a New Class of High Performance Photoinitiators: Blue Led Induced Polymerization of Methacrylates in Thin and Thick Films. *Macromolecules* **2017**, *50*, 6911–6923.